Frontiers in Bioscience Landmark

Front. Biosci. (Landmark Ed) **2022**; 27(12): 321
https://doi.org/10.31083/j.fbl2712321

Original Research

Determining the Role of SGLT2 Inhibition with Dapagliflozin in the Development of Diabetic Retinopathy

Lakshini Y. Herat[1,*,†], Jennifer R. Matthews[1,†], Wei E. Ong[1], Elizabeth P. Rakoczy[2], Markus P. Schlaich[3,4,5,‡], Vance B. Matthews[1,‡]

[1]Dobney Hypertension Centre, School of Biomedical Science – Royal Perth Hospital Unit, University of Western Australia, 6009 Crawley, WA, Australia
[2]Department of Molecular Ophthalmology, University of Western Australia, 6009 Crawley, WA, Australia
[3]Dobney Hypertension Centre, School of Medicine – Royal Perth Hospital Unit, University of Western Australia, 6009 Crawley, WA, Australia
[4]Department of Cardiology, Royal Perth Hospital, 6000 Perth, WA, Australia
[5]Department of Nephrology, Royal Perth Hospital, 6000 Perth, WA, Australia
*Correspondence: lakshini.weerasekera@uwa.edu.au (Lakshini Y. Herat)
†These authors contributed equally.
‡These authors contributed equally.
Academic Editor: Riccardo Nevola
Submitted: 22 July 2022 Revised: 14 November 2022 Accepted: 22 November 2022 Published: 12 December 2022

Abstract

Background: Diabetic retinopathy (DR) is a major cause of blindness globally. Sodium Glucose Cotransporter-2 (SGLT2) inhibitors have been demonstrated to exert cardiorenal protection in patients with diabetes. However, their potential beneficial effect on DR is less well studied. The aim of the present study was to determine the effects of the SGLT2 inhibition with Dapagliflozin (DAPA) on DR in well-characterised DR mouse models and controls. **Methods**: Dapagliflozin was administered to mice with and without diabetes for 8 weeks via their drinking water at 25 mg/kg/day. Urine glucose levels were measured weekly and their response to glucose was tested at week 7. After 8 weeks of treatment, eye tissue was harvested under terminal anaesthesia. The retinal vasculature and neural structure were assessed using immunofluorescence, immunohistochemistry and electron microscopy techniques. **Results**: Dapagliflozin treated DR mice exhibited metabolic benefits reflected by healthy body weight gain and pronounced glucose tolerance. Dapagliflozin reduced the development of retinal microvascular and neural abnormalities, increased the beneficial growth factor FGF21 (Fibroblast Growth Factor 21). We highlight for the first time that SGLT2 inhibition results in the upregulation of SGLT1 protein in the retina and that SGLT1 is significantly increased in the diabetic retina. **Conclusions**: Blockade of SGLT2 activity with DAPA may reduce retinal microvascular lesions in our novel DR mouse model. In conclusion, our data demonstrates the exciting future potential of SGLT1 and/or SGLT2 inhibition as a therapeutic for DR.

Keywords: diabetic retinopathy; diabetes; Akimba; mouse models; sodium glucose cotransporters; SGLT2 inhibitors; SGLT1; Dapagliflozin; Sotagliflozin; retinal vasculature

1. Introduction

Diabetes mellitus is a chronic metabolic disease characterised by hyperglycemia that accounts for 9.9% of the all-cause mortality worldwide, with approximately five million deaths attributable to diabetes mellitus in 2017 alone [1]. The impact of diabetes mellitus on quality of life is amplified by macrovascular and particularly microvascular complications associated with the disease. The most common complications in diabetes mellitus is diabetic retinopathy (DR) which is the leading cause of preventable vision loss in working-age adults [2]. Clinically, DR has two principal stages [3,4]. The initial non-proliferative DR (NPDR) phase is characterised by retinal microvascular changes such as pericyte loss, basement membrane thickening, formation of microaneurysms and intraretinal microvascular abnormalities. The more serious proliferative DR (PDR) stage is characterised by the development of new blood vessels (neovascularisation) on the surface of the retina. This in turn leads to fibrovascular changes and tractional retinal detachment, a common cause of associated blindness [5]. Persistent hyperglycemia, hypertension, microalbuminuria and renal disease are all risk factors associated with the development of DR [6–8]. The two major pillars of DR treatment are anti-angiogenic agents and laser photocoagulation. However, with the transient effects of the anti-angiogenic agents and their inefficacy in a third of patients, alongside the detrimental side effects of mild vision loss and reduced night vision with laser therapy [5], it is necessary to develop more effective therapies and identify novel therapeutic targets for DR. New therapeutic approaches that adopt a holistic view for the treatment of DR beyond regulating glucose homeostasis are warranted.

The entry of glucose into cells is regulated by facilitative glucose transporters (GLUTs) and sodium-dependent glucose cotransporters (SGLTs). Of SGLTs, SGLT1 and

SGLT2 are frequently investigated in a range of disease settings [9], as they play key roles in the transport of glucose and sodium across the brush border membrane of intestinal and renal cells [10]. SGLT2 inhibitors have been developed based on the anti-diabetic action initiated by inhibiting renal glucose reabsorption thereby increasing urinary glucose excretion [11]. As demonstrated by several large-scale clinical trials, SGLT2 inhibitors are now recognised to be capable of altering a range of metabolic and biochemical parameters thereby exerting cardio-renal protection in diabetic and non-diabetic individuals [12,13].

SGLT1 is mainly responsible for glucose absorption in the small intestine and for reabsorption of the part of the glucose load filtered in the kidney. Therefore, in addition to SGLT2 inhibition, SGLT1 inhibition is considered an additional target to achieve maintenance of good glycaemic control and improvement of renal dysfunction [14,15]. Interestingly and importantly in the context of DR, expression of SGLT1 and SGLT2 has recently been reported in the eye and the retina by us and others [16–18]. Given the encouraging findings from clinical studies in regards to SGLT2 inhibitor mediated protection from microvascular disease, specifically in the kidney, it appears plausible that similar benefits may extend to the retinal microvasculature. Relevant investigations are therefore warranted to establish a potential role of this therapeutic approach for DR. Here, we used SGLT2 inhibition in mouse models with retinal and neural damage associated with retinopathy and DR [19–21].

2. Materials and Methods

2.1 Mice and Genotyping

As model systems, we utilized the Kimba, Akita and Akimba mouse models. The Kimba mouse model (trVEGF029) transiently overexpresses human vascular endothelial growth factor in photoreceptors and demonstrates neovascular changes associated with DR without a hyperglycemic background [22]. These DR associated changes occur at the age of 3–4 weeks postnatally [19,22]. The Akita (*Ins2*Akita) mouse is a naturally occurring diabetic model that carries a dominant mutation in the insulin 2 gene. Male heterozygous Akita mice develop hyperglycaemia as early as 4 weeks of age and demonstrate some mild features of DR after 12 weeks of age [20]. By crossing Akita and Kimba mice, the Akimba (*Ins2*AkitaVEGF+/–) mouse model is generated, which combines the retinopathy features of the Kimba mouse with the hyperglycaemic background of the Akita mouse [21]. The Akimba mouse model displays hallmark retinal microvascular and neural abnormalities representative of human DR including microaneurysms, tortuous vessels, venous beading, vasodilation, capillary non-perfusion, increased retinal vascular leakage, edema, neovascularization, retinal layer alterations and thinning [21,23–25]. Some of these features develop in 8 to 9-week-old young Akimba mice (microaneurysms, severe capillary nonperfusion, haemorrhages, vascular leakage and tortuous retinal vessels) [21,24]. This model is a highly relevant model for the study of retinal vascular disease and in our study, we investigated ~7-week-old animals with the aim of evaluating the effect of DAPA in the prevention or slowing of the development of DR.

Using the Wizard Genomic DNA Purification Kit (catalogue #A1120, Promega, Madison, WI, USA) DNA was isolated from tail clippings. Genotyping of Kimba mice was carried out as described previously [22,25]. As described by Vagaja *et al*. [26] Akita mice were genotyped for the *Ins2* gene. Akimba mice were genotyped by using protocols for both Kimba and Akita mice.

2.2 Animals

All experimental and animal handing activities were performed at the Royal Perth Hospital animal holding facility or the Harry Perkins Institute for Medical Research animal holding facility (Perth, Western Australia, Australia) in accordance with the guidelines of institutional Animal Ethics Committee and ARVO statement for the Use of Animals in Ophthalmic and Vision Research. Animal ethics was approved by both the Royal Perth Hospital Animal Ethics Committee (R537/17-20; approved: 15/08/17) and Harry Perkins Institute for Medical Research Animal Ethics Committee (AE141/2019; approved: 12/02/19). Specific pathogen-free ~7-week-old male C57BL6/J, Kimba, Akita and Akimba mice were obtained from the Animal Resources Centre (Perth, Western Australia, Australia).

Mice were housed under a 12-hour light/dark cycle, at 21 $\pm$ 2 °C and were given a standard chow diet (Specialty Feeds, Glen Forrest, WA, Australia) with free access to food and drinking water. Following a 7-day acclimatization period, the SGLT2 inhibitor Dapagliflozin (DAPA; catalogue #A-0840, Ark Pharma Scientific Limited, China; 25 mg/kg/day), dual SGLT1 and 2 inhibitor Sotagliflozin (SOTAG; HY-15516/CS-1069, Med Chem Express, Princeton, NJ, USA; 25 mg/kg/day) or vehicle (dimethylsulfoxide) was administered to the mice via drinking water for 8 weeks. Drinking water containing the inhibitor or vehicle was freshly prepared and replenished on a weekly basis. Urine glucose levels were measured (Keto-Diastix; catalogue #2883, Bayer, Leverkusen, Germany) before treatment to confirm the phenotype of animals and 1-week post-treatment to establish the development of glucosuria induced by treatment. On a weekly basis, mice were weighed and consumed water volumes were measured.

In a separate set of experiments, Akimba mice were treated with the SGLT2 inhibitor Empagliflozin (EMPA; catalogue #H-020496, Ark Pharma Scientific Limited, China; 25 mg/kg/day) or vehicle for a period of 8 weeks via drinking water. Drinking water containing the inhibitor or vehicle was freshly prepared and replenished on a weekly basis. At the end of week 8, mice were euthanized and eye tissue was processed for histological analysis of SGLT1 protein expression.

2.3 Intraperitoneal Glucose Tolerance Test (GTT)

Glucose tolerance testing (GTT) was performed at the end of 7 weeks of treatment after 5 hours of fasting. Blood glucose levels were measured before (0 minutes) and 15, 30, 45, 60 and 90 minutes after intraperitoneal administration of 25% glucose solution at 1 g/kg body weight. All GTT test results higher than 33.3 mmol/L could not be determined due to glucometer limitations and were plotted as 33.3 mmol/L.

2.4 Specimen Collection

At the end of the experiment, mice were fasted for 5 hours with free access to treatment water. Animals were deeply anesthetized using isoflurane inhalation. Blood samples were collected using cardiac puncture and placed on ice immediately. Fasting blood glucose was measured using the Accu-Chek Performa blood glucose monitoring system (product ID: 2581627, Roche Diagnostics, North Ryde, Australia). Blood samples were centrifuged, serum collected and stored at –80 °C. Eyes were enucleated and cleaned to remove all muscle and connective tissue. The right eye was collected into 10% buffered paraformaldehyde for histology while the left eye was fixed in ice-cold 10% buffered paraformaldehyde for 2 hours at 4 °C in preparation for retinal vascular assessment. The optic nerve tissue was collected into glutaraldehyde and was processed to obtain semi-thin transverse sections for electron microscopy.

2.5 Evaluation of the Retinal Vasculature

Retinal flat mounts were prepared and analyzed with modification to a previously published method [27]. In brief, fully dissected retinas from the left eye were washed twice in 1× phosphate buffered saline (PBS) and were permeabilized for two hours at room temperature in PBS-BSA-Triton-X solution (1× PBS, 1% Bovine Serum Albumin (BSA), 1% Triton-X) followed by washing in Wash Buffer (1× PBS, 0.5% Triton-X) for five times. Retinas were treated with Isolectin GS-IB4 overnight at 4 °C (1:100 in Wash Buffer) with specificity for alpha-galactosylated glycoprotein residues on vascular endothelial cells and macrophages (Griffonia Simplicifolia Lectin I (GSL I); isolectin B4; catalog #B1205-5, Biotinylated; Vector Laboratories, Burlingame, CA, USA). Subsequently, the retinas were washed five times using 1× PBS and secondary antibody Cy3-Streptavidin (catalogue #PA43001, 1:500 in 1× PBS; GE Healthcare, Amersham, UK) was added and incubated for five hours in the dark at room temperature. Stained retinas were washed five times in 1× PBS, flat-mounted and cover-slipped with VECTASHIELD HardSet Anti-fade Mounting Medium (catalogue #H-1400, Vector Laboratories, Burlingame, CA, USA).

2.6 Section Preparation with Hematoxylin and Eosin and SGLT1 Immunohistochemistry

Enucleated eyes were fixed in 4% paraformaldehyde for 24 hours, placed in 70% ethanol overnight, followed by wax embedding and collection of 5 μm sections. A series of sections were stained with hematoxylin and eosin (H&E). Additional sections were deparaffinised in xylene (2 × 10 minutes) and rehydrated in 100% (2 × 5 minutes), 95% (1 × 1 minute) and 70% ethanol (1 × 3 minutes). Slides were then placed under running tap water for 5 minutes. Antigen retrieval was carried out by placing tissues in pre-heated EDTA (pH 8.5; Sigma–Aldrich, Sydney, Australia) and further heating with micropower for 5 minutes. Slides were washed in PBS + 0.1% Tween (2 × 5 minutes) and sections were outlined using a paraffin pen. Sections were treated with 3% H_2O_2 for 10 minutes, washed with PBS + 0.1% Tween (2 × 5 minutes) and blocked with 5% Fetal Bovine Serum in PBS + 0.1% Tween for 1 hour at 4 °C in a humidified chamber. Slides were incubated with a combination of Rabbit anti-SGLT1 antibodies (catalogue #ab14685, Abcam, Melbourne, Australia and Novus Biologicals, Melbourne, Australia, respectively) in 5% Fetal Bovine Serum in PBS + 0.1% (1:180 and 1:100, respectively), overnight at 4 °C in a humidified chamber and washed with PBS + 0.1% Tween (3 × 5 minutes). Retinal sections were incubated with donkey anti-rabbit horseradish peroxidase (HRP; cat #NA934V Thermo Fisher Scientific, Victoria, Australia) in PBS + 0.1% Tween (1:500) for 1 hour. Detection was performed using Ultraview Universal DAB (3, 3'-Diaminobenzidine) detection kit (Product no. 760-500, Ventana Medical Systems, Tucson, AZ, USA) according to the manufacturer's instructions, followed by counterstaining of nuclei with Gill's haematoxylin. Slides were washed, dehydrated, cleared and mounted using Dibutylphthalate Polystyrene Xylene (DPX; catalogue #06522, Sigma–Aldrich, Sydney, Australia).

2.7 Section Preparation with Glial Fibrillary Acid Protein (GFAP)

For GFAP immunohistochemistry, 5 μm wax sections were mounted onto charged slides and incubated for 60 minutes at 60 °C. The immunohistochemistry was performed on a Benchmark Ultra™ staining module (material no. 05342716001, Ventana Medical Systems, Tucson, AZ, USA) using recommended reagents. In brief, the slides were deparaffinized using EZ prep (Product no. 950–102) followed by epitope retrieval (Cell conditioner no. 1, pH 8.5, Product no. 950–124) at 95 °C for 36 minutes. Sections were incubated with monoclonal mouse GFAP antibody (Clone GF2 1:3000) (catalogue #M0761, DAKO, Glostrup, Denmark) for 32 minutes at 36 °C. UltraView Universal DAB detection (Product no. 760–500) was used for visualization of the bound primary antibody using the manufacturer's recommend protocol. The slides were then

counterstained with Hematoxylin and bluing reagent prior to dehydration in graded alcohols.

2.8 Retinal Whole Mount Section Imaging and Analysis

Retinal whole-mounts were imaged from the vitreous side using the inverted fluorescent microscopic system Nikon Eclipse Ti (Nikon, Tokyo, Japan) with a digital camera CoolSNAP HQ2 (Photometrics, Tucson, AZ, USA) linked to a computer running the image analysis software 'NIS-Elements Advanced Research' V4.0 (Nikon, Tokyo, Japan). Overlapping high-resolution images of the entire retinas were captured using the 4× objective. Images were merged to construct a montage of the retina. The generated low magnification photomontages were used to count the number of retinal vascular lesions such as microaneurysms, intra retinal microvascular abnormalities (IRMA) within 2000 μm radius from the optic nerve head (NIS-Elements Advanced Research, Nikon, Tokyo, Japan). Representative areas of retinal vascular lesions were captured in the z-plane in 2 μm steps. The z-stacks were compiled into a focused image representing all superficial, intermediate and deep capillary layers.

Brightfield imaging of retinal sections stained with H&E, SGLT1 or GFAP were conducted using the microscopic system Nikon Eclipse Ti (Nikon, Tokyo, Japan) with a digital camera CoolSNAP HQ2 (Photometrics, Tucson, AZ, USA) linked to a computer running the image analysis software 'NIS-Elements Advanced Research' (Nikon, Tokyo, Japan).

H&E-stained retinal sections were scanned for overall gross anatomy followed by morphometric analysis. Morphometric measurements included counting the cells in the ganglion cell layer. Retinal ganglion cells were quantified by counting ganglion cells in a 100 μm linear distance in the mid retinal region. In addition, overall retinal thickness and specific nuclear layer thickness was measured.

Retinal sections were screened for GFAP expression in Müller cells across the length of each retinal section. Müller cell projections spanning beyond the ganglion cell layer were considered for Müller cell gliosis. Each retinal section was screened in the mid retinal region in a linear manner. At least two retinal sections per eye was assessed.

The mean SGLT1 staining intensity score of stained retinal sections was calculated in counterstained retinal tissue. The SGLT1 staining intensity for each mouse retina was scored on a scale of 0–3 (0 = no staining; 1 = low; 2 = intermediate; 3 = high).

2.9 Assessment of Optic Neuropathy

Left and right optic nerves from Akimba mice were processed for ultrastructural studies. Tissues were initially fixed in 2.5% glutaraldehyde at room temperature for 24 hours and then rinsed in cacodylate buffer. Optic nerve preparations were post-fixed in 1% osmium tetroxide, dehydrated through graded Alcohols and Propylene Oxide and infiltrated with epoxy resin on a Lynx tissue processor. Semi-thin sections were obtained and stained with toluidine blue for screening regions of the tissue block face to obtain ultra-thin sections of optic nerve tissue. Ultra-thin sections were obtained at 100 nm and stained with uranyl acetate and Reynold's Lead citrate. Sections were imaged using a JEOL 1200EX Transmission Electron Microscope at 120 kV (JEOL, Tokyo, Japan). A series of images were obtained from the outer edge and from the middle of the cross sectioned optic nerve tissue representing the 'outer' and 'inner' regions, respectively. The frequency of axons with structural anomalies such as interrupted axonal flow, accumulation of mitochondria, dense tubular lamellae and multi vesicular bodies was assessed in axonal profiles.

2.10 Enzyme-Linked Immunosorbent Assays

Serum was analyzed for Fibroblast Growth Factor 21 (FGF21) using the Duoset human FGF21 enzyme-linked immunosorbent assay (ELISA) kit (Cat# DY2539, R&D systems, Inc., Minneapolis, MN, USA) according to the manufacturer's respective instructions.

2.11 Statistical Analysis

All morphometric data were analyzed using two-tailed Student's *t*-test and $p \leq 0.05$ was considered as a significant threshold.

3. Results

3.1 SGLT2 Inhibition with DAPA Promoted Glucosuria in Non-Diabetic C57BL/6 and Kimba Mice

Both C57BL/6 (WT) and Kimba models lack the hyperglycemic background and hence acts as an internal control for the effectiveness of the SGLT2 inhibitor DAPA used in this study. Prior to treatment, urine glucose testing via dipstick method showed 0 mmol/L glucose in both C57Bl/6 and Kimba strains and $\geq$111 mmol/L in the diabetic Akita and Akimba mice (data not shown). As anticipated, the consumption of DAPA in drinking water at a concentration of 25 mg/kg/day, resulted in marked glucose secretion in the urine of non-diabetic C57BL/6 (Fig. 1A) and Kimba mice (Fig. 1B) while remaining at 0 mmol/L in mice receiving vehicle. Urine glucose levels of the diabetic Akita and Akimba mice were $\geq$111 mmol/L regardless of treatment. Furthermore, all C57BL/6, Kimba, Akita and Akimba mice displayed normal responses to touch, smooth and healthy body coats, bright eyes and normal posture throughout the 8 weeks of DAPA treatment.

3.2 Treatment with DAPA Prevented the Failure to Thrive in Diabetic Mice

Over the 8 weeks of treatment, non-diabetic C57BL/6 (WT) and Kimba mice gained weight at similar rates irrespective of treatment (Fig. 2A,C). Diabetic Akita and Akimba mice typically show poor weight gain, a hallmark of the failure to thrive phenotype in these animals. At the

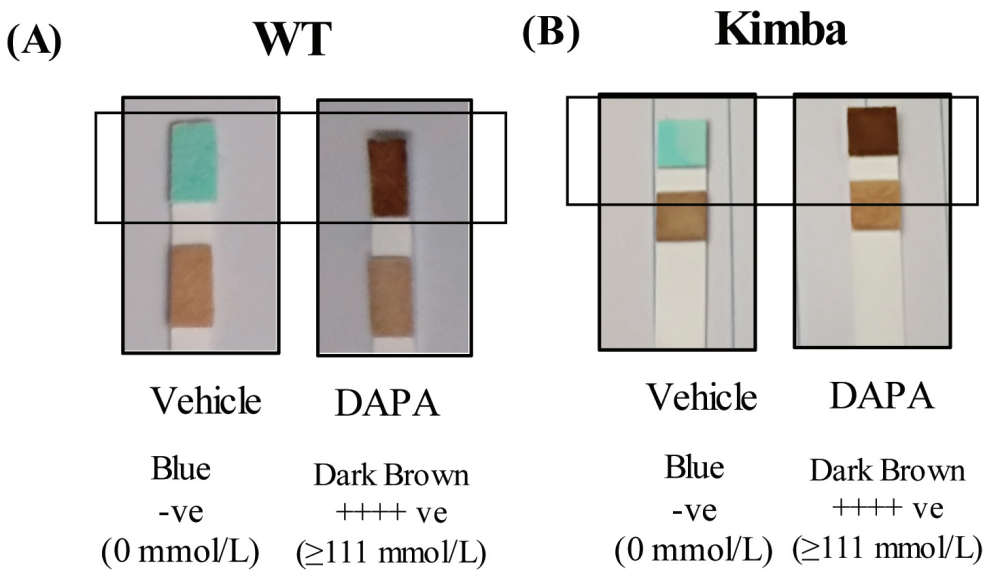

Fig. 1. SGLT2 inhibition with DAPA promotes glucosuria in non-diabetic wild-type C57BL/6 and Kimba mice. Representative image of glucose levels in the urine in (A) wild-type C57BL/6 and (B) Kimba mice treated with vehicle or DAPA (25 mg/kg); Blue = 0 mmol/L glucose, Dark brown ≥111 mmol/L glucose. SGLT2, Sodium glucose cotransporter 2; DAPA, Dapagliflozin.

end of 8 weeks of treatment both Akita and Akimba mice receiving DAPA exhibited significantly increased body weight gain when compared to their counterparts receiving vehicle (Fig. 2B,D).

3.3 Treatment with DAPA Significantly Reduced Fasting Blood Glucose Levels in Diabetic Mice

Following 8 weeks of treatment, there was no difference in the fasting blood glucose levels of C57BL/6 mice (WT) receiving either vehicle (14.4 ± 1.8 mmol/L) or DAPA (13.1 ± 1.4 mmol/L) (Fig. 3A). Kimba mice also had similar fasting blood glucose levels upon receiving either vehicle (10.7 ± 0.4 mmol/L) or DAPA (9.4 ± 0.6 mmol/L) for 8 weeks (Fig. 3C). The fasting blood glucose levels of both Akita (18.5 ± 2.7 mmol/L) and Akimba (15.1 ± 1.6 mmol/L) mice after 8 weeks of DAPA treatment were significantly lower than Akita (29.8 ± 1.7 mmol/L) and Akimba (27.0 ± 3.8 mmol/L) treated with vehicle (Fig. 3B,D, respectively).

3.4 DAPA Treatment Reduced Glucose Intolerance in Diabetic Akimba Mice

As shown in Fig. 4, a GTT was performed to evaluate glucose tolerance 7 weeks after DAPA treatment. When compared to Kimba mice treated with vehicle, treatment with DAPA significantly decreased average blood glucose levels 30 minutes after glucose challenge (Fig. 4A). This significant decrease continued up to 90 minutes after glucose challenge. However, in Akimba mice treated with DAPA, the average blood glucose levels were significantly lower prior to glucose challenge (0 minutes) and continued to be lower than vehicle treated mice during the course of 90 minutes after glucose challenge (Fig. 4B).

3.5 Retinal Vascular Benefits of SGLT2 Inhibition with DAPA in Mice with DR

Upon fluorescent microscopic examination, there were no discernable differences in the retinal vasculature of vehicle or DAPA treated C57BL/6J (WT) and Akita mice (**Supplementary Fig. 1**). Furthermore, retinal vascular abnormalities such as capillary dropouts or microaneurysms indicative of diabetic retinopathy were absent in both groups of diabetic Akita mice (**Supplementary Fig. 1C,D**). In both models with retinopathy (Kimba) and DR (Akimba), the development of retinal vascular lesions was evident as previously published [16,21–23,25]. Therefore, the number of vascular lesions were counted in Kimba and Akimba mice to determine the effect of SGLT2 inhibition on the retinal vascular features. There was no appreciable difference between the number of lesions in Kimba mice receiving DAPA (32.3 ± 2.9 lesions) or vehicle (30.6 ± 2.9 lesions) (Fig. 5A,C). However, in Akimba mice treated with DAPA (53.5 ± 2.3 lesions), there were significantly less lesions observed compared to Akimba mice treated with vehicle (66.7 ± 3.8 lesions) (Fig. 5B,D). This result is highly novel.

3.6 Neural Retinal Benefits of SGLT2 Inhibition with DAPA in Mice with DR

The complex pathology of DR affects both vascular and neural tissue. The characteristics of neurodegeneration are well-described in animal models of DR [28]. We exam-

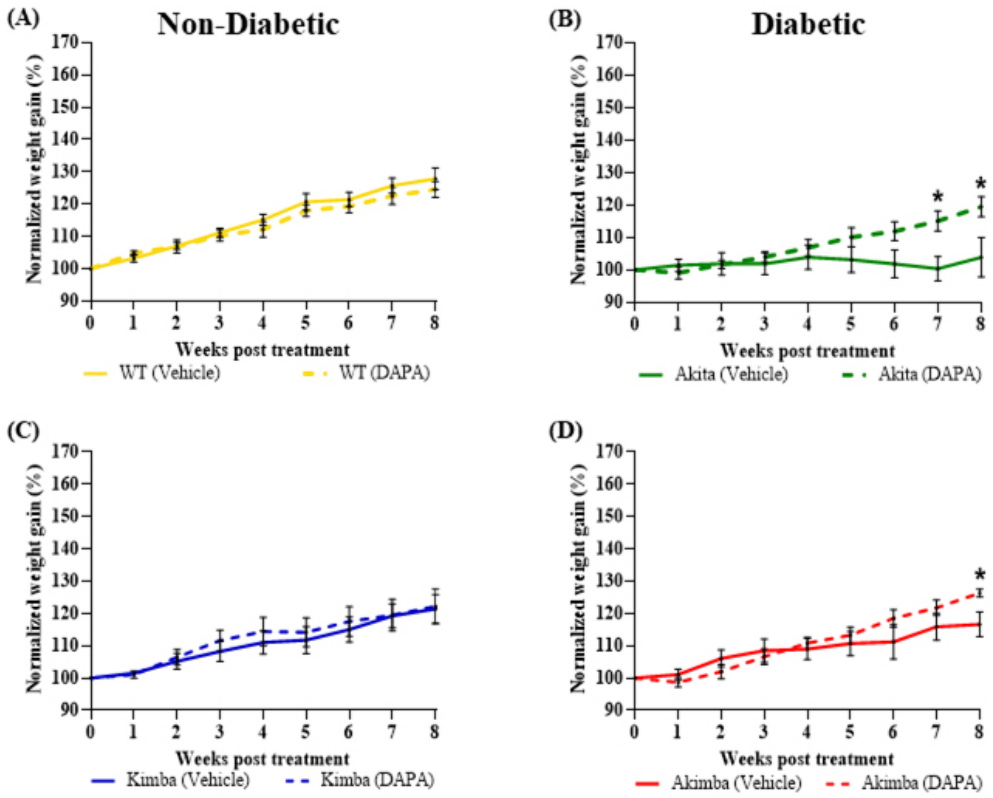

Fig. 2. Effect of SGLT2 inhibition on body weight in non-diabetic and diabetic mice treated with DAPA. Graphs show the normalized body weight percentage during 8 weeks of treatment with DAPA or vehicle in (A) wild-type C57BL/6, (B) Akita, (C) Kimba and (D) Akimba mice. *$p \leq 0.05$; data represented as mean ± SEM of 5-6 mice per group. SGLT2, Sodium glucose cotransporter 2; DAPA, Dapagliflozin.

ined the neural retina in each group by H&E staining and observed that in vehicle treated Akimba mice (Fig. 6A,B), retinal cells appeared disorganised, intercellular space increased and retinal capillaries often penetrated the generally avascular outer retinal layers (Fig. 6A,B: *yellow arrows*). In particular, rosette formations (Fig. 6A,B: *yellow boxes*) was noted in 40% of the vehicle treated mice. In contrast, DAPA treatment preserved the well-structured, intact and tightly arranged manner of plexiform and nuclear layers and minimised abnormal blood vessel transgression which causes damage to the outer layers of the retina (Fig. 6C,D).

Neurodegeneration characterised by loss of neural cell populations accompanying thinning and alterations of retinal layers are well documented [29]. Measurements of mid-retinal thickness in non-diabetic C57B6/J (Wild-Type; WT) and diabetic Akimba mice treated with vehicle or DAPA are shown in Fig. 7. Overall, the retinal thickness in WT mice with or without SGLT2 inhibitor treatment appeared normal (Fig. 7A) and did not show any significant difference when measured (Fig. 7B). When compared to WT mice, the retinal thickness was significantly reduced in diabetic Akimba mice regardless of treatment (WT vs Akimba (Vehicle) Full retina, INL (inner nuclear layer), ONL (outer nuclear layer); *$p \leq 0.05$ and WT vs Akimba (DAPA) Full retina, INL, ONL; *$p \leq 0.05$). However, in DAPA treated Akimba mice (Fig. 7C; *right panel* and D) the retina was protected from degeneration when compared to vehicle treated Akimba mice (Fig. 7C; *left panel* and D). Akimba mice with DAPA treatment showed an overall significantly thicker retina, specifically the INL (Fig. 7C; *right panel* and D). There was no significant difference in the retinal ganglion cell number between vehicle and DAPA treated Akimba groups (**Supplementary Fig. 2**).

Gliosis of Müller cells can be present in various retinal pathologies and is a distinct feature of DR [30]. Reactive Müller cells are characterised by the expression of GFAP in the fine projections of Müller cells spanning across the neural retina indicating the gliosis process [31]. In vehicle treated Akimba mice, radial Müller cell projections indicating gliosis of Müller cells were noted (Fig. 8A,B; *black closed-arrows*), while the GFAP expression in DAPA treated mice were limited to astrocytes and the endfeet of Müller cells (Fig. 8C and D; *black open-arrows*) located in the NFL and GCL.

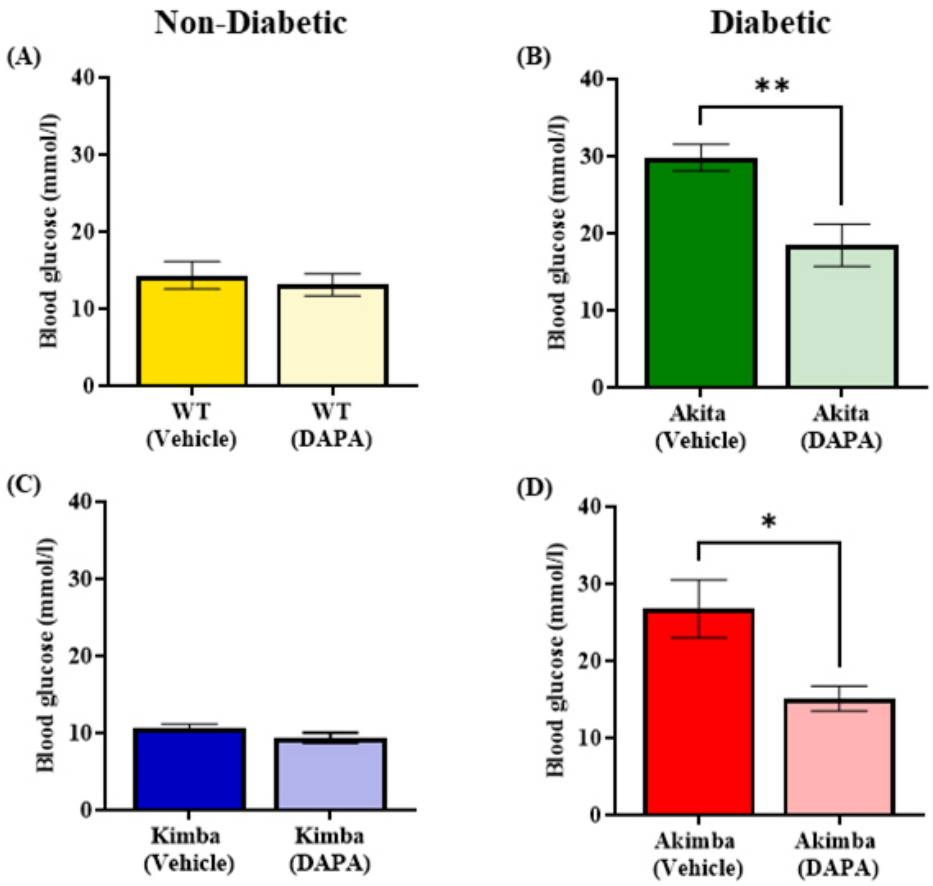

Fig. 3. Effect of SGLT2 inhibition on blood glucose in non-diabetic and diabetic mice treated with DAPA. Graphs show fasting blood glucose levels after 8 weeks of treatment with DAPA or vehicle in (A) wild-type C57BL/6, (B) Akita, (C) Kimba and (D) Akimba mice. *$p \leq 0.05$, **$p \leq 0.005$; data represented as mean ± SEM of 5–6 mice per group. SGLT2, Sodium glucose cotransporter 2; DAPA, Dapagliflozin; WT, Wild-type.

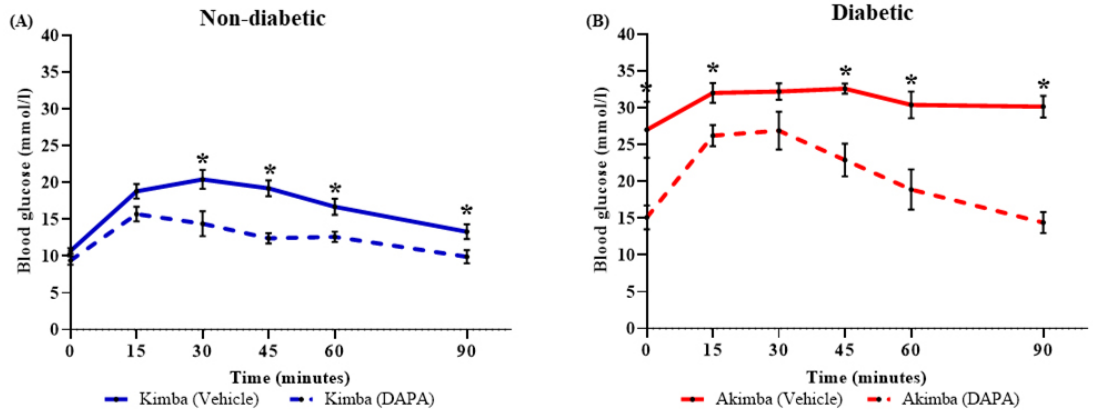

Fig. 4. SGLT2 inhibition with DAPA reduced glucose intolerance in diabetic Akimba mice. Blood glucose was measured at 0, 15, 45, 60, and 90 minutes after glucose challenge in (A) non-diabetic Kimba and (B) diabetic Akimba mice. *$p \leq 0.05$; data represented as mean ± SEM of 5–6 mice per group. SGLT2, Sodium glucose cotransporter 2; DAPA, Dapagliflozin.

3.7 Treatment with the SGLT2 Inhibitor DAPA Prevented Optic Neuropathy in Akimba Mice

Transmission electron microscopic analysis of Akimba optic nerves showed myelinated fibers forming axonal bundles. The axoplasms of the fibers were light and contained mitochondria, microtubules, and neurofilaments. In both inner and outer optic nerve regions, DAPA treated mice (Fig. 9B,D) showed more compact bundles

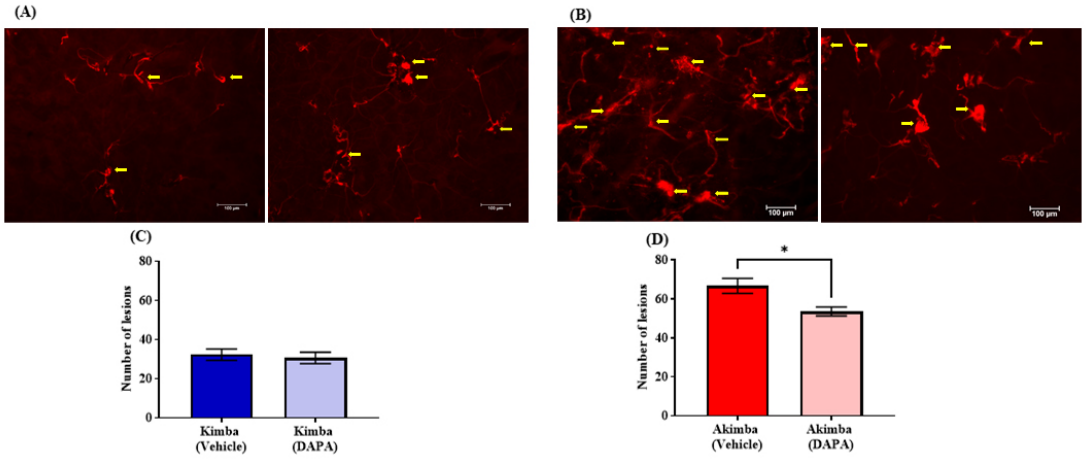

Fig. 5. Treatment with DAPA reduced retinal microvascular lesions in diabetic Akimba mice. Representative areas of isolectin-B4 and Cy-3 stained vasculature from (A) Kimba and (B) Akimba mice treated with vehicle or DAPA. Quantification of retinal vascular lesions in (C) Kimba and (D) Akimba mice treated with vehicle versus DAPA. A reduced numbers of retinal microvascular lesions (*yellow arrows*) were observed in (D) Akimba mice treated with DAPA when compared to vehicle treated mice. $*p \leq 0.05$; data represented as mean ± SEM of 3–5 mice per group. Scale bar 100 μm; DAPA, Dapagliflozin.

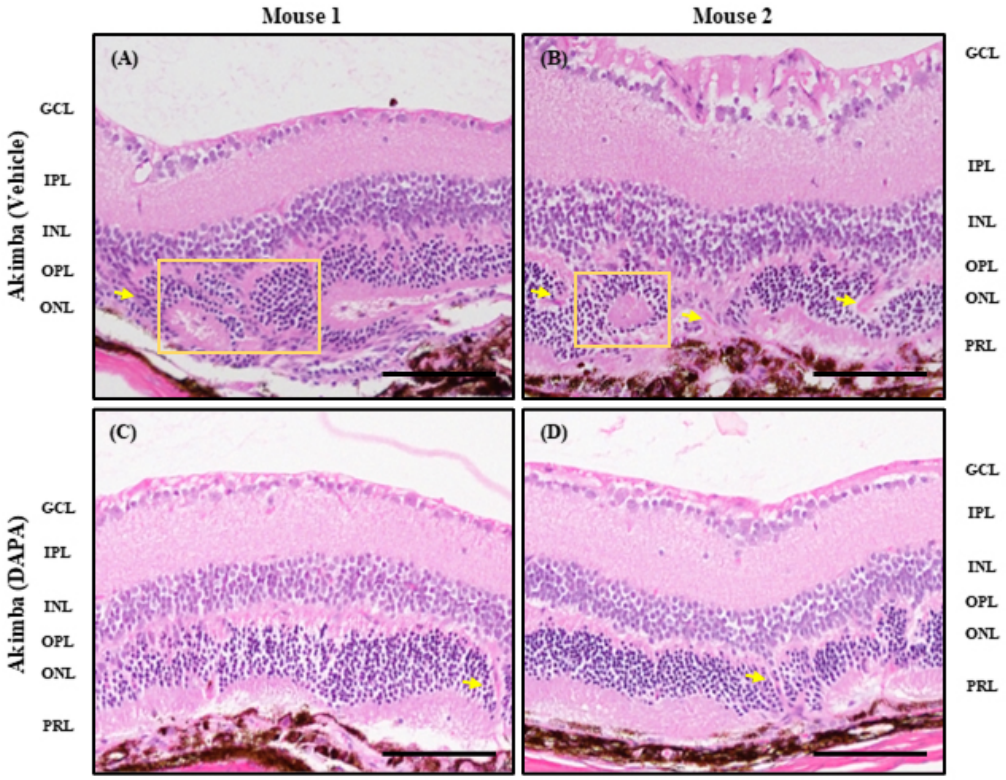

Fig. 6. Treatment with DAPA improved retinal neural damage in diabetic Akimba mice. Light micrographs of H&E stained retinal sections of Akimba mice treated with vehicle (A,B) or DAPA (C,D). Akimba mice treated with vehicle showing increased number of blood vessels transgressing the normally blood vessel-free photoreceptor cell layers (A–D; *yellow arrows*) and rosette formation (A,B; *yellow boxes*). Treatment with DAPA reduced retinal neural damage (C,D). n = 3–4 mice per group. GCL, ganglion cell layer; IPL, inner plexiform layer; INL, inner nuclear layer; OPL, outer plexiform layer; ONL, outer nuclear layer; PRL, photo receptor layer. Scale bar: 50 μm.

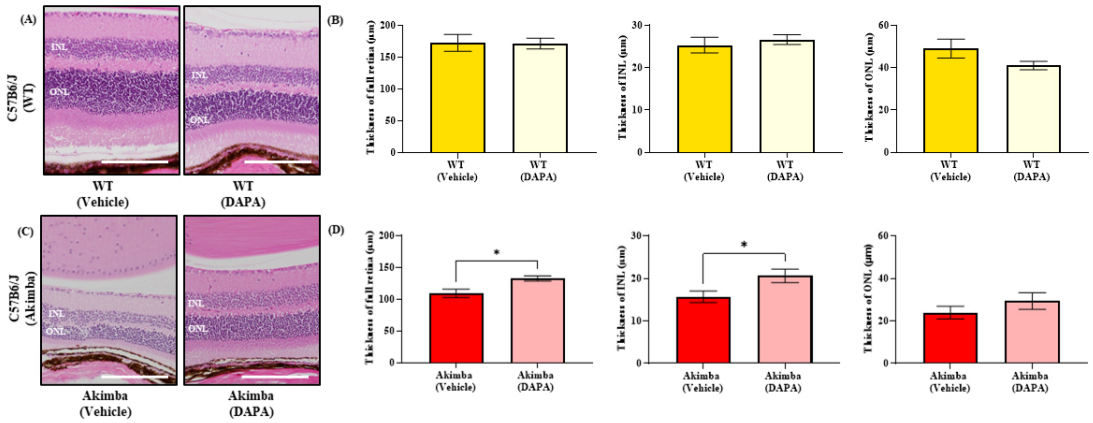

Fig. 7. Treatment with DAPA preserved retinal nuclear layers in diabetic Akimba mice. Thickness of the total retina, outer nuclear layer and inner nuclear layer was performed in the mid retina of non-diabetic C57B6/J WT (A,B) and diabetic Akimba mice (C,D) treated with Vehicle or DAPA. *$p \leq 0.05$ between Akimba vehicle (*dark red bars*) and Akimba DAPA (*light red bars*) mice. Data represented as mean ± SEM of 3–5 mice per group. INL, inner nuclear layer; ONL, outer nuclear layer; DAPA, Dapagliflozin and WT, Wild-Type. Scale bar: 50 μm.

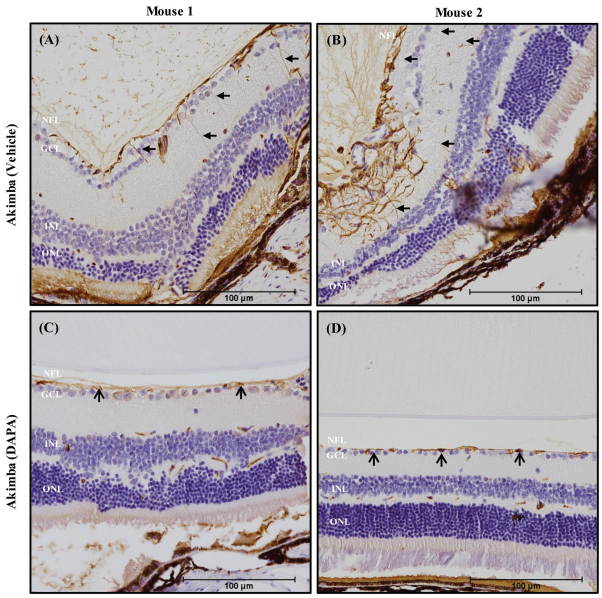

Fig. 8. Müller cell gliosis in the mid-retinal region was reduced with DAPA treatment in Akimba mice. Paraffin sections were stained for GFAP expression and visualised in the Müller cell projections spanning across retinal layers in the mid-retinal region. Vehicle treated Akimba mice (A,B) showed Müller cell gliosis (*black closed-arrows*) while DAPA treated mice (C,D) showed GFAP expression confined to astrocytes and Müller cell end-feet (*black open-arrows*). Data represented from n = 5 mice per group. DAPA, Dapagliflozin; NFL, Nerve fiber layer; GCL, ganglion cell layer; INL, inner nuclear layer and ONL, outer nuclear layer. Scale bar: 100 μm.

of myelinated fibres when compared to vehicle treated mice (Fig. 9A,C). Furthermore, thinly myelinated fibers, nude axons and collapsed myelin sheaths were observed more frequently in Akimba mice receiving the vehicle compared to Akimba mice receiving DAPA. Overall, DAPA treatment resulted in a more stable architecture of the optic nerve.

3.8 Effects of SGLT2 Inhibition with DAPA on Circulating FGF21 Levels

Diabetic Akita mice (Fig. 10A) treated with DAPA (59.8 ± 27.0 pg/mL) had a higher serum FGF21 concentration than Akita mice treated with vehicle (8.2 ± 4.0 pg/mL). Furthermore, DAPA treatment significantly elevated FGF21 serum levels in Akimba mice (55.8 ± 14.6 pg/mL) in comparison to Akimba mice receiving vehicle (17.6 ± 5.5 pg/mL) (Fig. 10B).

3.9 Effects of SGLT2 Inhibition on SGLT1 Expression in the Retina

Our recent studies show that diabetic Akimba mice have increased SGLT2 expression in the eye compared to non-diabetic Kimba mice [16]. The SGLT family member, SGLT1, is an integral membrane protein responsible for the mechanism of active glucose transport and it may be expressed in the eye/retina [17,32]. We then asked the question whether SGLT2 inhibition may result in SGLT1 upregulation to act as a compensatory mechanism. Interestingly, when compared to vehicle treated mice (Fig. 11A,B), inhibition of SGLT2 with either EMPA (Fig. 11C,E) or DAPA (Fig. 11D,F) increased SGLT1 in the retinas of diabetic Akimba mice. The overall SGLT1 expression was confined to the plexiform layers of the retina. It was consistently observed that the increased intensity of SGLT1 in the EMPA (Fig. 11C) and DAPA (Fig. 11D) treated groups were mainly limited to the inner and outer plexiform layers where the neuronal synaptic contacts occur in the retina.

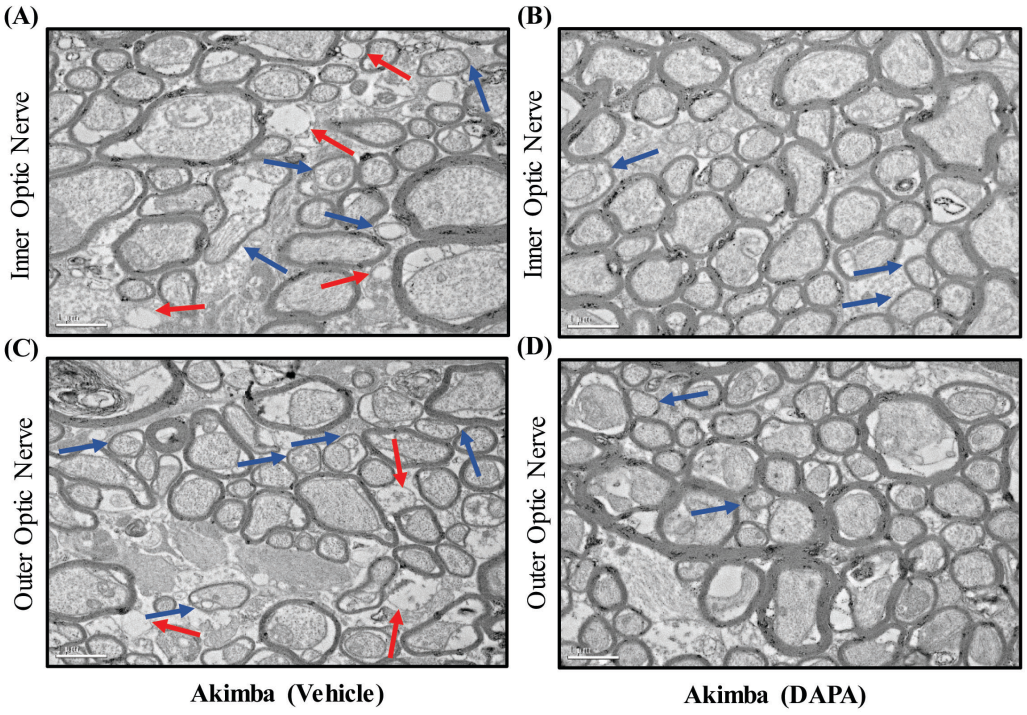

Fig. 9. Treatment with DAPA improved optic neuropathy in diabetic Akimba mice. Transmission electron microscopy of the inner (A,B) and outer (C,D) regions of the optic nerve of Akimba mice treated with vehicle (A,C) or DAPA (B,D) for 8 weeks. Key features; thinly myelinated fibers (*blue arrows*) and nude axons (*red arrows*). Scale bar 1 μm; DAPA, Dapagliflozin.

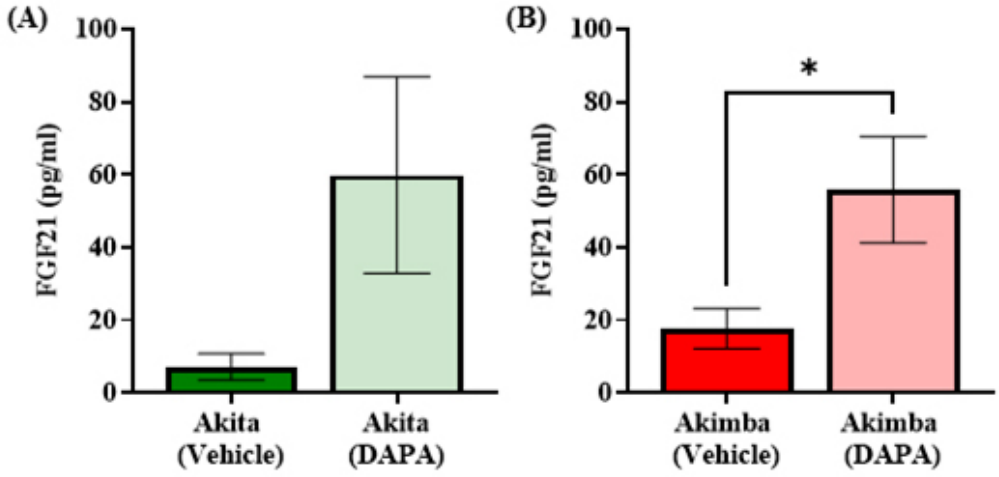

Fig. 10. Treatment with DAPA increased the beneficial growth factor FGF21 in diabetic Akita and Akimba mice. Graphs show FGF21 levels after 8 weeks of treatment with DAPA or vehicle in (A) Akita and (B) Akimba mice. *$p \leq 0.05$; data represented as mean $\pm$ SEM of 4–7 mice per group. FGF21, Fibroblast Growth Factor 21; DAPA, Dapagliflozin.

3.10 SGLT1 Protein Levels are Significantly Increased in Diabetic Akimba and Akita Mouse Models

Using a novel immunohistochemistry method, we have demonstrated for the first time that SGLT1 protein levels are significantly increased in the retinas of diabetic Akimba mice (Fig. 12B,C) when compared to non-diabetic Kimba mice (Fig. 12A,C). When compared to non-diabetic Kimba mice, the diabetic Akimba mice displayed increased SGLT1 expression which was confined to the nerve fiber, inner plexiform, outer plexiform and photoreceptor layers (Fig. 12B). This phenomenon appears to not only be confined to the retina. When compared to C57BL/6J (WT) mice, type 1 diabetic Akita mice also showed increased SGLT1 expression in pancreatic islet cells (Fig. 13).

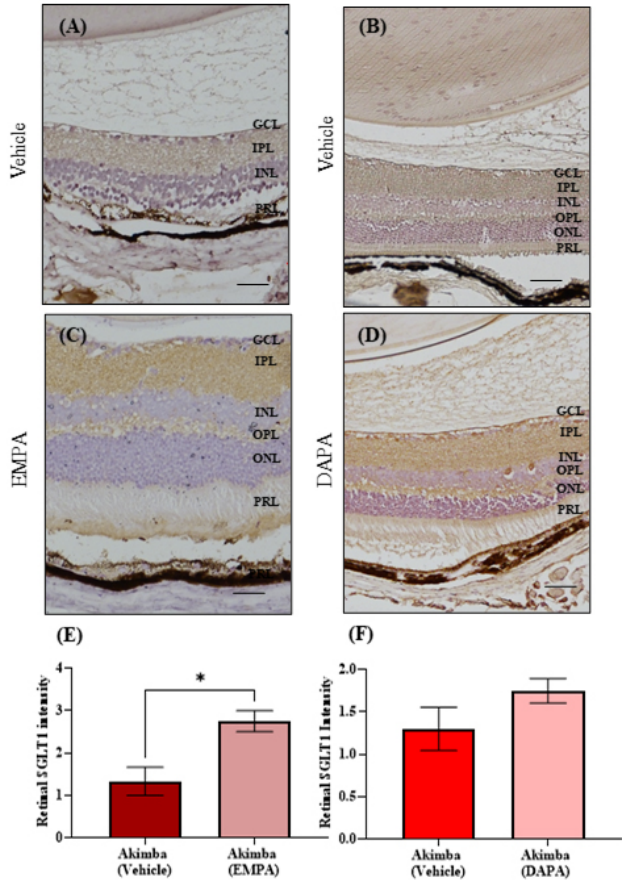

Fig. 11. SGLT2 inhibition promoted over expression of SGLT1 protein levels in the retinas of diabetic Akimba mice. Light micrographs of SGLT1 stained retinal sections of (A,B) Akimba vehicle, (C) Akimba EMPA and (D) Akimba DAPA treated mice. Graphs show SGLT1 levels after 8 weeks of treatment in Akimba mice with vehicle versus (E) EMPA or (F) DAPA mice. $*p \leq 0.01$; data represented as mean $\pm$ SEM of 3–5 mice per group. GCL, ganglion cell layer; IPL, inner plexiform layer; INL, inner nuclear layer; OPL, outer plexiform layer; ONL, outer nuclear layer; PRL, photo receptor layer. Scale bar 100 μm; SGLT1, Sodium glucose cotransporter 1; SGLT2, Sodium glucose cotransporter 2; EMPA, Empagliflozin; DAPA, Dapagliflozin.

3.11 Dual Inhibition of SGLT1 and 2 Significantly Upregulated SGLT1 Protein Levels in the Retinas of Akimba Mice with DR

Given that SGLT2 inhibition results in SGLT1 upregulation, we sought to assess the effect of dual SGLT1 and 2 inhibition on SGLT1 expression with Sotgliflozin (SOTAG) in diabetic Akimba mice. Interestingly, when compared to vehicle treated Akimba mice (Fig. 14A), SOTAG treated mice showed a significant increase in the SGLT1 protein level (Fig. 14B,C). The increased SGLT1 protein expression in SOTAG treated Akimba mice was predominantly observed in the inner plexiform layer (Fig. 14B).

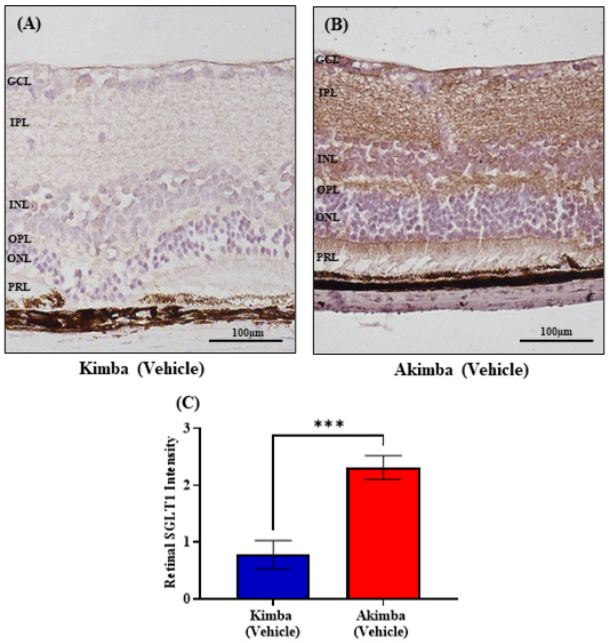

Fig. 12. Diabetic retinopathy promotes retinal SGLT1 protein expression in diabetic Akimba mice. Light micrographs of SGLT1 stained retinal sections of (A) non-diabetic Kimba and (B) diabetic Akimba mice treated with vehicle. (C) Graph shows SGLT1 levels after 8 weeks of vehicle treatment in Kimba vs Akimba mice. $***p \leq 0.001$; data represented as mean $\pm$ SEM of 8–9 mice per group. GCL, ganglion cell layer; IPL, inner plexiform layer; INL, inner nuclear layer; OPL, outer plexiform layer; ONL, outer nuclear layer; PRL, photo receptor layer. Scale bar: 100 μm; DAPA, Dapagliflozin; SGLT1, Sodium glucose cotransporter 1.

4. Discussion

Diabetes is one of the fastest growing chronic metabolic diseases globally and the leading cause of preventable blindness. As such, therapies effectively tackling underlying cardiovascular and renal complications and the related ophthalmic conditions like DR are urgently required. There have been studies conducted on the effect of SGLT2 inhibitors such as EMPA [33] and Ipragliflozin [34] for the treatment of DR in diabetic rodents. However, there is limited data from either animal models or clinical trials regarding the effects of SGLT2 inhibition on DR in type 1 diabetes [16]. In addition to our findings, a single study [35] has reported the protective effects of the SGLT2 inhibitor DAPA on DR in the setting of type 1 diabetes. Interestingly, our group is the first to uncover DAPA mediated reductions in retinal microvascular lesions in type 1 diabetic mice.

As expected, the normalized weight gain of non-diabetic WT and Kimba mice were similar in both DAPA and vehicle treated groups. The failure to thrive phenotype indicated by poor weight gain is a hallmark feature

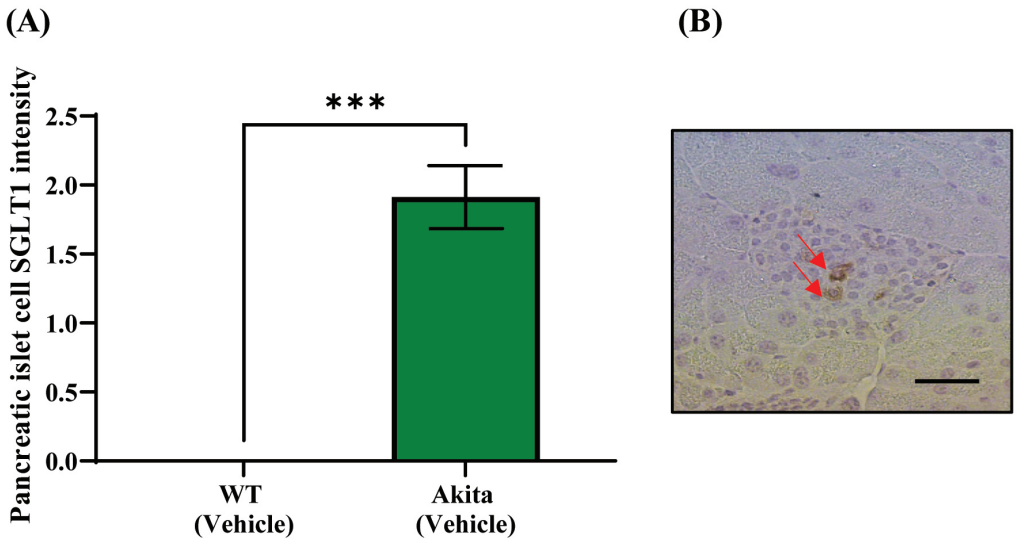

Fig. 13. Increased SGLT1 expression in the pancreata of diabetic Akita mice. (A) Quantitation of SGLT1 positive islet cells; intensity scale (0 = no staining; 1 = low staining; 2 = intermediate staining; 3 = high intensity). Representative image of (B) SGLT1immunohistochemistry in the islet cells of diabetic Akita mice (*red arrows: brown SGLT1 positive cells*). ***$p \leq 0.0001$; data represented as mean ± SEM of 4–5 mice per group. Scale bar: 100 μm; SGLT1, Sodium glucose cotransporter 1; WT, Wild-type.

of uncontrolled type 1 diabetes in mice [20,36–38]. The significant weight loss and muscle waste is possibly due to catabolic effects (accelerated protein catabolism and diminished protein synthesis) of insulin deficiency, as well as volume depletion associated with the osmotic diuresis in type 1 diabetes [36]. This may have a significant impact on subsequent survival of animals in long-term studies. Interestingly, this was circumvented with DAPA, where both diabetic Akita and Akimba mice with DAPA treatment exhibited an increase in weight gain post 3 weeks of treatment when compared to vehicle treated mice. Therefore, it is promising that DAPA prevents the weight loss associated with type 1 diabetes (Fig. 2). Furthermore, all mice exhibited normal behavior and showed no weight loss due to SGLT2 inhibition suggesting that SGLT2 inhibition does not promote detrimental side effects. Interestingly, we have previously shown that SGLT2 inhibition promotes sympathoinhibition in type 1 diabetic mice and as mice treated with DAPA do not lose weight, this indicates that sympathoinhibition is not associated to weight changes [39].

Similar to other SGLT2 inhibitor studies conducted in type 1 diabetic mice [40,41] the glucose-lowering effects of DAPA treatment was evident by the significant reduction in fasting blood glucose levels in both Akita and Akimba (DAPA) mice in comparison to their vehicle treated counterparts (Fig. 3). It is clear from studies by Han *et al.* [42] that DAPA reduces glucose levels by being markedly more active at inhibiting SGLT2 compared to SGLT1. In fact, DAPA is 207 time more potent at reducing SGLT2 compared to SGLT1.

A large number of clinical studies have reported that DAPA and a range of other SGLT2 inhibitors, reduce the risk of major adverse cardiovascular events and prevent the progression of kidney diseases [43], suggesting that SGLT2 inhibition may exert beneficial effects on both macro- and micro-vascular complications in diabetic patients. A recent study showed that the treatment of type 2 diabetic patients with SGLT2 inhibitors EMPA or DAPA slowed the progression of DR in comparison with sulfonylurea, which occurs independently of its effect on glycemic control [44]. In addition, SGLT2 inhibitors might be associated with lowering the risk of DR compared with DPP4 inhibitors [45].

As characterised previously [21], the Akimba mouse showed characteristic retinopathic changes which were associated with the retinal vasculature and the neural structure. Our investigations further add to the growing body of evidence associated with the beneficial role of SGLT2 inhibitors by demonstrating the protective effect of DAPA on retinal vascular and neural architecture (Figs. 5,6,7,8). In diabetic rats, treatment with DAPA reduced retinal capillary dilation, arteriole remodelling, retinal hypertrophy and ganglion cell degradation [46]. A separate study in diabetic rats showed ipragliflozin prevented irregularity of the retinal outer nuclear layer [34]. In addition, it has been shown that the SGLT2 inhibitor EMPA significantly attenuated early manifestations of non-proliferative DR, such as retinal microaneurysms and showed relatively normal overall retinal thickness in db/db mice. However, the nerve fiber and ganglion cell layers were disorganized in these animals [33]. Furthermore, in diabetic db/db mice, DAPA effectively reduced the formation of acellular capillaries and improved the electroretinogram response [47]. Hu *et al.* [35] demonstrated in STZ-induced diabetic mice that DAPA treatment improved the thickness of the inner nuclear and outer nu-

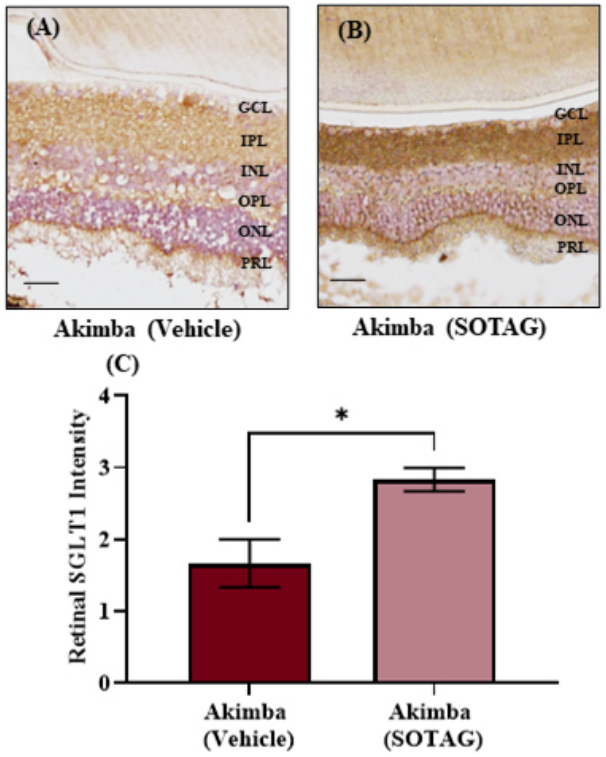

Fig. 14. Dual inhibition of SGLT1 and 2 with SOTAG upregulates SGLT1 protein levels in the retinas of diabetic Akimba mice. Light micrographs of SGLT1 stained retinal sections of (A) Akimba Vehicle and (B) Akimba SOTAG treated mice. (C) Graph shows SGLT1 levels after 8 weeks of treatment in Akimba mice with vehicle versus SOTAG. *$p \leq 0.05$; data represented as mean $\pm$ SEM of 3 mice per group. GCL, ganglion cell layer; IPL, inner plexiform layer; INL, inner nuclear layer; OPL, outer plexiform layer; ONL, outer nuclear layer; and PRL, photo receptor layer. Scale bar: 100 μm; SGLT1, Sodium glucose cotransporter 1; SOTAG, Sotagliflozin.

clear layers of the neural retina by reducing apoptosis. Our findings demonstrate that DAPA played a similar role in reducing DR associated early retinal microvascular lesions (Fig. 5), decreased morphological modifications occurring in the outer neural layers (Fig. 6) and preserved the overall retinal thickness (Fig. 7). As shown by many studies using SGLT2 inhibitors [33,34,45–49], the DR associated protective effects of DAPA in Akimba mice is potentially mediated by the improvement in long-term glycaemic control (8 weeks). However, recent studies have shown DAPA induced reductions in oxidative stress [46] and inflammation [46,47] improved retinal vascular and neural pathology in DR. Therefore, future studies should be carried out in the Akimba model to establish the role of oxidative stress and inflammation mitigated by SGLT2 inhibition.

Another classical feature of retinal neurodegeneration is glial activation. We have shown that administration of DAPA decreased glial activation indicated by reduced GFAP expression in the Akimba mouse retina (Fig. 8). Comparable to our findings, Hanaguri *et al.* [48] showed that tofogliflozin treatment also prevented Müller cell gliosis. Hyperglycaemia induced retinal hyperoxia is a well-established mechanism of retinal Müller cell activation. Furthermore, Müller cell activation can dysregulate retinal blood flow, compromise retinal barrier function and initiate deleterious inflammatory process with the release of proinflammatory cytokines. The beneficial effect of SGLT2 inhibition on retinal glial cells may potentially lead to the recovery of the diabetes-induced retinal damage via improved glycaemic control and inflammation [33,48]. Taken together, large-scale prospective clinical studies are warranted to examine the effect of SGLT2 inhibition on the prevention of development and progression of DR.

Fibroblast Growth Factor 21 (FGF21) is a major metabolic regulator which has been shown to be elevated in various metabolic disturbances including type 2 diabetes and metabolic syndrome [50]. The rise in circulating FGF21 levels in type 2 diabetes and obese patients is due to its compensatory and protective role [50,51]. FGF21 has been studied extensively in diabetes and obesity and has been shown to decrease blood glucose and plasma insulin levels, as well as improving the lipid profile, which signifies its potential in treating type 2 diabetes. FGF21 has also been shown to act in an autocrine manner in order to protect the quality and function of the pancreatic β cells [8]. In our mechanistic study, we have shown increased FGF21 levels in both diabetic Akita and Akimba mice treated with DAPA (Fig. 10). Several studies have demonstrated the beneficial role of FGF21 in the setting of retinopathy. Fu *et al.* [52] demonstrated that FGF21 administration suppresses pathological ocular blood vessel growth in the retina and choroid in a mouse model of hypoxia-driven retinal neovascularization. Investigations carried out in STZ-diabetic mice and the Akita model has shown that the long-acting FGF21 analogue PF-05231023 restored photoreceptor structure and function, and reduced photoreceptor oxidative stress and inflammation [53]. In *in vitro* and *in vivo* models, FGF21 prevents VEGF-induced retinal vascular leakage by stabilizing vascular endothelial cell tight junctions and therefore, may have therapeutic potential for preventing or treating retinopathy and suppresses retinal neovascularization [54]. In addition, it is shown that increased FGF21 levels in the plasma and liver attenuated pathological neovascularization in murine Oxygen-Induced Retinopathy [55] and protected retinal neural activity in STZ-induced diabetes [56]. It has also been shown that in type 1 diabetic patients with retinopathy, FGF21 levels were significantly lower when compared to healthy individuals [57]. Given the relevance of the Akimba mouse model in the context of DR, it is of utmost importance to not only determine the role of FGF21 in the pathogenesis of DR in this mouse model but also to determine the effect of SGLT2 inhibitors on FGF21 levels.

A burning question for the field is whether SGLT2 inhibition promotes compensatory SGLT1 upregulation [58]. To the best of our knowledge, a single study suggests that SGLT1 activity is increased with SGLT2 inhibition. According to Rieg *et al*. [59], during SGLT2 inhibition, the glucose load to the SGLT1-expressing S2/S3 segments of the proximal tubule is enhanced and a compensatory increase in SGLT1 mediated transport occurs. In our current study, we showed that both DAPA and EMPA promoted an upregulation of SGLT1 protein in the retina of diabetic Akimba mice (Fig. 11). Interestingly, EMPA promoted the largest SGLT1 elevation. It is critical for further studies to be conducted to substantiate these findings and to explore whether combined SGLT1 and 2 inhibition may be even more beneficial both in terms of achieving glucose control and providing protection from microvascular damage.

In this context, our study is highly novel as we are the first to show that dual SGLT1 and 2 inhibition with SOTAG significantly increased SGLT1 expression in the diabetic retina (Fig. 14). Together with our demonstration of elevated retinal expression of SGLT1 in the type 1 diabetic Akimba mice compared to their non-diabetic parental Kimba mice (Fig. 12) it is pertinent to consider sole SGLT1 therapy in the future for the prevention or reduction of the severity of DR.

5. Conclusions

In conclusion, our study is the first to show that DAPA administered to type 1 diabetic Akimba mice not only increases beneficial FGF21 levels but also improves retinal structure and reduces the number of microvasculature lesions. Further research is needed to determine how the dual SGLT1 and 2 inhibitor SOTAG affects retinal health.

Availability of Data and Materials

The datasets used and/or analyzed during the current study are available from the corresponding author on reasonable request.

Author Contributions

Conceptualization—LYH, VBM, MPS and EPR; formal analysis—LYH, JRM, WEO and VBM; funding acquisition—LYH, VBM and MPS; investigation—LYH, JRM, WEO, VBM and MPS; writing-original draft—LYH, JRM and VBM; writing-review and editing—LYH, JRM, WEO, MPS, EPR and VBM. All authors have read and agreed to the published version of the manuscript.

Ethics Approval and Consent to Participate

Animal ethics was approved by both the Royal Perth Hospital Animal Ethics Committee (R537/17-20; approved: 15/08/17) and Harry Perkins Institute for Medical Research Animal Ethics Committee (AE141/2019; approved: 12/02/19).

Acknowledgment

We thank Dr. Aaron Magno (University of Western Australia, Western Australia) and Ms. Moira Hibbs (Research Centre, Royal Perth Hospital, Western Australia) for technical assistance. Authors thank Animal Resources Centre (Murdoch, Western Australia) and the Bioresources, Harry Perkins Institute of Medical Research (Nedlands, Western Australia) for providing animal care services. We also thank Dr. Anmol Rijhumal, Mr. Bob Mirzai and Mr. Terry Kop (Anatomical Pathology, PathWest Laboratory Medicine, Fiona Stanley Hospital, Murdoch, Western Australia) for assisting with GFAP immunohistochemistry.

Funding

This study was funded by the Royal Perth Hospital-Research Foundation WA (VM2018), Diabetes Australia Research Program (Y20G-MATV), Diabetes Research WA (DRWA-LHerat-2020) and Raine Medical Research Foundation, WA (Raine-LHerat-2020).

Conflict of Interest

The authors declare no conflict of interest.

Supplementary Material

Supplementary material associated with this article can be found, in the online version, at https://doi.org/10.31083/j.fbl2712321.

References

[1] Cho NH, Shaw JE, Karuranga S, Huang Y, da Rocha Fernandes JD, Ohlrogge AW, *et al*. IDF Diabetes Atlas: Global estimates of diabetes prevalence for 2017 and projections for 2045. Diabetes Research and Clinical Practice. 2018; 138: 271–281.

[2] Congdon N, Zheng Y, He M. The worldwide epidemic of diabetic retinopathy. Indian Journal of Ophthalmology. 2012; 60: 428.

[3] Grading diabetic retinopathy from stereoscopic color fundus photographs–an extension of the modified Airlie House classification. ETDRS report number 10. Early Treatment Diabetic Retinopathy Study Research Group. Ophthalmology. 1991; 98: 786–806.

[4] Wilkinson CP, Ferris FL, Klein RE, Lee PP, Agardh CD, Davis M, *et al*. Proposed international clinical diabetic retinopathy and diabetic macular edema disease severity scales. Ophthalmology. 2003; 110: 1677–1682.

[5] Wang W, Lo ACY. Diabetic Retinopathy: Pathophysiology and Treatments. International Journal of Molecular Sciences. 2018; 19: 1816.

[6] Crimi S, Cipolli D, Infantone E, Infantone L, Lunetta M. Microalbuminuria and severity of diabetic retinopathy in type 1 diabetic patients: association and relationship with some risk factors. Diabetes & Metabolism. 1995; 21: 440–445.

[7] Hirsch IB, Brownlee M. Beyond hemoglobin A1c–need for additional markers of risk for diabetic microvascular complications. JAMA. 2010; 303: 2291–2292.

[8] Klein R, Knudtson MD, Lee KE, Gangnon R, Klein BEK. The Wisconsin Epidemiologic Study of Diabetic Retinopathy: XXII the twenty-five-year progression of retinopathy in persons with type 1 diabetes. Ophthalmology. 2008; 115: 1859–1868.

[9] Sano R, Shinozaki Y, Ohta T. Sodium–glucose cotransporters: Functional properties and pharmaceutical potential. Journal of Diabetes Investigation. 2020; 11: 770–782.
[10] Wright EM. The Intestinal Na+/Glucose Cotransporter. Annual Review of Physiology. 1993; 55: 575–589.
[11] Chao EC, Henry RR. SGLT2 inhibition — a novel strategy for diabetes treatment. Nature Reviews Drug Discovery. 2010; 9: 551–559.
[12] Xiang B, Zhao X, Zhou X. Cardiovascular benefits of sodium-glucose cotransporter 2 inhibitors in diabetic and nondiabetic patients. Cardiovascular Diabetology. 2021; 20: 78.
[13] Dutka M, Bobiński R, Ulman-Włodarz I, Hajduga M, Bujok J, Pająk C, *et al*. Sodium glucose cotransporter 2 inhibitors: mechanisms of action in heart failure. Heart Failure Reviews. 2021; 26: 603–622.
[14] Lehmann A, Hornby PJ. Intestinal SGLT1 in metabolic health and disease. American Journal of Physiology-Gastrointestinal and Liver Physiology. 2016; 310: G887–G898.
[15] Song P, Onishi A, Koepsell H, Vallon V. Sodium glucose cotransporter SGLT1 as a therapeutic target in diabetes mellitus. Expert Opinion on Therapeutic Targets. 2016; 20: 1109–1125.
[16] Matthews J, Herat L, Rooney J, Rakoczy E, Schlaich M, Matthews VB. Determining the role of SGLT2 inhibition with Empagliflozin in the development of diabetic retinopathy. Bioscience Reports. 2022; 42: BSR20212209.
[17] Lim JC, Perwick RD, Li B, Donaldson PJ. Comparison of the expression and spatial localization of glucose transporters in the rat, bovine and human lens. Experimental Eye Research. 2017; 161: 193–204.
[18] Herat LY, Matthews VB, Rakoczy PE, Carnagarin R, Schlaich M. Focusing on Sodium Glucose Cotransporter-2 and the Sympathetic Nervous System: Potential Impact in Diabetic Retinopathy. International Journal of Endocrinology. 2018; 2018: 9254126.
[19] van Eeden PE, Tee LBG, Lukehurst S, Lai C, Rakoczy EP, Beazley LD, *et al*. Early Vascular and Neuronal Changes in a VEGF Transgenic Mouse Model of Retinal Neovascularization. Investigative Opthalmology & Visual Science. 2006; 47: 4638.
[20] Barber AJ, Antonetti DA, Kern TS, Reiter CE, Soans RS, Krady JK, *et al*. The Ins2Akita mouse as a model of early retinal complications in diabetes. Investigative Ophthalmology & Visual Science. 2005; 46: 2210-2218.
[21] Rakoczy EP, Rahman ISA, Binz N, Li C, Vagaja NN, de Pinho M, *et al*. Characterization of a Mouse Model of Hyperglycemia and Retinal Neovascularization. The American Journal of Pathology. 2010; 177: 2659–2670.
[22] Lai C. Generation of transgenic mice with mild and severe retinal neovascularisation. British Journal of Ophthalmology. 2005; 89: 911–916.
[23] Chaurasia SS, Lim RR, Parikh BH, Wey YS, Tun BB, Wong TY, *et al*. The NLRP3 Inflammasome may Contribute to Pathologic Neovascularization in the Advanced Stages of Diabetic Retinopathy. Scientific Reports. 2018; 8: 2847.
[24] McLenachan S, Magno AL, Ramos D, Catita J, McMenamin PG, Chen FK, *et al*. Angiography reveals novel features of the retinal vasculature in healthy and diabetic mice. Experimental Eye Research. 2015; 138: 6–21.
[25] Wisniewska-Kruk J, Klaassen I, Vogels IMC, Magno AL, Lai C, Van Noorden CJF, *et al*. Molecular analysis of blood–retinal barrier loss in the Akimba mouse, a model of advanced diabetic retinopathy. Experimental Eye Research. 2014; 122: 123–131.
[26] Vagaja NN, Chinnery HR, Binz N, Kezic JM, Rakoczy EP, McMenamin PG. Changes in Murine Hyalocytes are Valuable Early Indicators of Ocular Disease. Investigative Opthalmology & Visual Science. 2012; 53: 1445–1451.
[27] Weerasekera LY, Balmer LA, Ram R, Morahan G. Characterization of Retinal Vascular and Neural Damage in a Novel Model of Diabetic Retinopathy. Investigative Opthalmology & Visual Science. 2015; 56: 3721–3730.
[28] Barber AJ, Baccouche B. Neurodegeneration in diabetic retinopathy: Potential for novel therapies. Vision Research. 2017; 139: 82–92.
[29] Barber AJ, Gardner TW, Abcouwer SF. The Significance of Vascular and Neural Apoptosis to the Pathology of Diabetic Retinopathy. Investigative Opthalmology & Visual Science. 2011; 52: 1156–1163.
[30] Mizutani M, Gerhardinger C, Lorenzi M. Müller cell changes in human diabetic retinopathy. Diabetes. 1998; 47: 445–449.
[31] Feit-Leichman RA, Kinouchi R, Takeda M, Fan Z, Mohr S, Kern TS, *et al*. Vascular Damage in a Mouse Model of Diabetic Retinopathy: Relation to Neuronal and Glial Changes. Investigative Opthalmology & Visual Science. 2005; 46: 4281–4287.
[32] Rizzolo LJ. Glucose Transporters in Retinal Pigment Epithelium Development. In Tombran-Tink J, Barnstable CJ (ed) Ocular Transporters In Ophthalmic Diseases And Drug Delivery: Ophthalmology Research (pp. 185–199). Humana Press: Totowa, NJ. 2008.
[33] Gong Q, Zhang R, Wei F, Fang J, Zhang J, Sun J, *et al*. SGLT2 inhibitor-empagliflozin treatment ameliorates diabetic retinopathy manifestations and exerts protective effects associated with augmenting branched chain amino acids catabolism and transportation in db/db mice. Biomedicine & Pharmacotherapy. 2022; 152: 113222.
[34] Takakura S, Toyoshi T, Hayashizaki Y, Takasu T. Effect of ipragliflozin, an SGLT2 inhibitor, on progression of diabetic microvascular complications in spontaneously diabetic Torii fatty rats. Life Sciences. 2016; 147: 125–131.
[35] Hu Y, Xu Q, Li H, Meng Z, Hao M, Ma X, *et al*. Dapagliflozin Reduces Apoptosis of Diabetic Retina and Human Retinal Microvascular Endothelial Cells Through ERK1/2/cPLA2/AA/ROS Pathway Independent of Hypoglycemic. Frontiers in Pharmacology. 2022; 13: 827896.
[36] Breyer MD, Böttinger E, Brosius FC, Coffman TM, Harris RC, Heilig CW, *et al*. Mouse Models of Diabetic Nephropathy. Journal of the American Society of Nephrology. 2005; 16: 27–45.
[37] Kim AK, Hamadani C, Zeidel ML, Hill WG. Urological complications of obesity and diabetes in males and females of three mouse models: temporal manifestations. American Journal of Physiology-Renal Physiology. 2020; 318: F160–F174.
[38] Matthews JR, Schlaich MP, Rakoczy EP, Matthews VB, Herat LY. The Effect of SGLT2 Inhibition on Diabetic Kidney Disease in a Model of Diabetic Retinopathy. Biomedicines. 2022; 10: 522.
[39] Herat LY, Ward NC, Magno AL, Rakoczy EP, Kiuchi MG, Schlaich MP, *et al*. Sodium glucose co-transporter 2 inhibition reduces succinate levels in diabetic mice. World Journal of Gastroenterology. 2020; 26: 3225–3235.
[40] Miyata KN, Zhao S, Wu C, Lo C, Ghosh A, Chenier I, *et al*. Comparison of the effects of insulin and SGLT2 inhibitor on the Renal Renin-Angiotensin system in type 1 diabetes mice. Diabetes Research and Clinical Practice. 2020; 162: 108107.
[41] Yaginuma H, Banno R, Sun R, Taki K, Mizoguchi A, Kobayashi T, *et al*. Peripheral combination treatment of leptin and an SGLT2 inhibitor improved glucose metabolism in insulin-dependent diabetes mellitus mice. Journal of Pharmacological Sciences. 2021; 147: 340–347.
[42] Han S, Hagan DL, Taylor JR, Xin L, Meng W, Biller SA, *et al*. Dapagliflozin, a Selective SGLT2 Inhibitor, Improves Glucose Homeostasis in Normal and Diabetic Rats. Diabetes. 2008; 57: 1723–1729.
[43] McGuire DK, Shih WJ, Cosentino F, Charbonnel B, Cherney DZI, Dagogo-Jack S, *et al*. Association of SGLT2 Inhibitors with

Cardiovascular and Kidney Outcomes in Patients with Type 2 Diabetes. JAMA Cardiology. 2021; 6: 148–158.
[44] Cho EH, Park S, Han S, Song JH, Lee K, Chung Y. Potent Oral Hypoglycemic Agents for Microvascular Complication: Sodium-Glucose Cotransporter 2 Inhibitors for Diabetic Retinopathy. Journal of Diabetes Research. 2018; 2018: 6807219.
[45] Chung YR, Ha KH, Lee K, Kim DJ. Effects of sodium-glucose cotransporter-2 inhibitors and dipeptidyl peptidase-4 inhibitors on diabetic retinopathy and its progression: A real-world Korean study. PLoS ONE. 2019; 14: e0224549.
[46] Taher MM, Shoukry HS. Protective Effect of Sodium-Glucose Co-Transporter 2 Inhibitor (Dapagliflozin) on Diabetic Retinopathy in Streptozotocin Induced Diabetes in Rats. The Medical Journal of Cairo University. 2019; 87: 465–470.
[47] Luo Q, Leley SP, Bello E, Dhami H, Mathew D, Bhatwadekar AD. Dapagliflozin protects neural and vascular dysfunction of the retina in diabetes. BMJ Open Diabetes Research & Care. 2022; 10: e002801.
[48] Hanaguri J, Yokota H, Kushiyama A, Kushiyama S, Watanabe M, Yamagami S, *et al*. The Effect of Sodium-Dependent Glucose Cotransporter 2 Inhibitor Tofogliflozin on Neurovascular Coupling in the Retina in Type 2 Diabetic Mice. International Journal of Molecular Sciences. 2022; 23: 1362.
[49] Eid SA, O'Brien PD, Hinder LM, Hayes JM, Mendelson FE, Zhang H, *et al*. Differential Effects of Empagliflozin on Microvascular Complications in Murine Models of Type 1 and Type 2 Diabetes. Biology. 2020; 9: 347.
[50] Chavez AO, Molina-Carrion M, Abdul-Ghani MA, Folli F, DeFronzo RA, Tripathy D. Circulating Fibroblast Growth Factor-21 is Elevated in Impaired Glucose Tolerance and Type 2 Diabetes and Correlates with Muscle and Hepatic Insulin Resistance. Diabetes Care. 2009; 32: 1542–1546.
[51] Chen C, Cheung BMY, Tso AWK, Wang Y, Law LSC, Ong KL, *et al*. High plasma level of fibroblast growth factor 21 is an independent predictor of type 2 diabetes: a 5.4-year population-based prospective study in Chinese subjects. Diabetes Care. 2011; 34: 2113–2115.
[52] Fu Z, Gong Y, Liegl R, Wang Z, Liu C, Meng SS, *et al*. FGF21 Administration Suppresses Retinal and Choroidal Neovascularization in Mice. Cell Reports. 2017; 18: 1606–1613.
[53] Fu Z, Wang Z, Liu C, Gong Y, Cakir B, Liegl R, *et al*. Fibroblast Growth Factor 21 Protects Photoreceptor Function in Type 1 Diabetic Mice. Diabetes. 2018; 67: 974–985.
[54] Tomita Y, Fu Z, Wang Z, Cakir B, Cho SS, Britton W, *et al*. Long-Acting FGF21 Inhibits Retinal Vascular Leakage in In Vivo and In Vitro Models. International Journal of Molecular Sciences. 2020; 21: 1188.
[55] Tomita Y, Ozawa N, Miwa Y, Ishida A, Ohta M, Tsubota K, *et al*. Pemafibrate Prevents Retinal Pathological Neovascularization by Increasing FGF21 Level in a Murine Oxygen-Induced Retinopathy Model. International Journal of Molecular Sciences. 2019 Nov 23;20(23):5878.
[56] Tomita Y, Lee D, Miwa Y, Jiang X, Ohta M, Tsubota K, Kurihara T. Pemafibrate Protects Against Retinal Dysfunction in a Murine Model of Diabetic Retinopathy. International Journal of Molecular Sciences. 2020; 21: 6243.
[57] Rosell Rask S, Krarup Hansen T, Bjerre M. FGF21 and glycemic control in patients with T1D. Endocrine. 2019; 65: 550–557.
[58] Martinez-Martin FJ, Jimenez-Martin N, Sablon-Gonzalez N. SGLT1 does compensate for SGLT2 inhibition. European Heart Journal - Cardiovascular Pharmacotherapy. 2016; 2: 256–256.
[59] Rieg T, Masuda T, Gerasimova M, Mayoux E, Platt K, Powell DR, *et al*. Increase in SGLT1-mediated transport explains renal glucose reabsorption during genetic and pharmacological SGLT2 inhibition in euglycemia. American Journal of Physiology-Renal Physiology. 2014; 306: F188–F193.